TECHNICAL PAPER

Analytical methods used for low temperature Cu–Cu wafer bonding process evaluation

B. Rebhan · S. Tollabimazraehno · G. Hesser · V. Dragoi

Abstract Metal wafer bonding is a well-established technology in the semiconductor industry. This technology gains more and more importance due to increasing market demands, particularly for three-dimensional integrated circuits and integration of complementary metal oxide semiconductor and microelectromechanical systems devices used in consumer electronics. Cu–Cu wafer bonding at low temperature is a very attractive process which can be used for both mechanical joints and electrical interconnects in wafer-level processes. In order to facilitate a permanent Cu–Cu bond at low temperature—in contrast to a typical ~400 °C Cu–Cu bonding temperature—the effect of material properties and bonding parameters has to be understood well. Therefore a comprehensive characterization including both, namely surface and interface analysis before and after wafer bonding of non-patterned Cu layers, respectively, is required in order to optimize the Cu–Cu metal wafer bonding process. Low temperature Cu–Cu bonding, namely ≤200 °C, of ~500 nm sputter-deposited Cu films was demonstrated and characterized. Selected analytical methods, such as transmission electron microscopy, Auger electron spectroscopy and electron backscatter diffraction, and their corresponding specimen preparation techniques for microstructure and elemental composition evaluation are introduced. Experimental results of surfaces and interfaces investigation (materials properties with high impact on their bonding behavior), such as the (i) surface roughness, (ii) Cu native oxide, (iii) Cu (surface) purity and (iv) Cu grain size, as well as the influence of the (vi) bonding temperature are presented.

1 Introduction

With the increased level of integration of electronic devices, wired global interconnections between different components, e.g. processor, memory or analogue integrated circuits (IC), became a bottleneck in increasing speed and operating frequencies. Therefore, besides scaling down the critical dimensions and developing new material combinations, also new integration schemes have to be developed. In general, three-dimensional (3D) packaging refers to various ways of stacking chips in the z-direction by (i) wire bonding them to a common substrate, (ii) package-on-package stacking, (iii) embedded chip stacking or (iv) direct connection with through silicon via (TSV). The 3D packaging method where at least two chips are connected with TSVs, is referred to as 3D integrated circuits (3D ICs). This integration scheme establishes a major reduction of the global interconnection length.

Within the 3D IC process flow the vertical integration for multi-layer device structures are facilitated using TSVs with either via-last, via-middle or via-first process and layer stacking (Chen and Tan 2011; Mounier et al. 2012).

During past decade the metal thermo-compression wafer bonding process emerged as crucial process enabling 3D ICs manufacturing. Since chemical mechanical polishing (CMP) yields metal surface roughness in the atomic range (Baudin et al. 2011; Moriceau et al. 2012) and diffusion

B. Rebhan (✉) · V. Dragoi
EV Group, DI E. Thallner 1, 4782 St. Florian am Inn, Austria
e-mail: b.rebhan@evgroup.com

S. Tollabimazraehno · G. Hesser
Center of Surface- and Nanoanalytics, Johannes Kepler
University, 4040 Linz, Austria

S. Tollabimazraehno
Christian Doppler Laboratory for Microscopic and Spectroscopic
Material Characterization, Linz, Austria

barrier layers were developed to prevent unwanted diffusion of fast-diffusing Cu into Si and Si dissolution in Cu (Istratova and Weberb 2002), the most attractive wafer bonding material combination is Cu–Cu (Chen et al. 2004). Besides the high electrical and mechanical thermal conductivity, the use of Cu is beneficial due to the existing infrastructure, no formation of Kirkendall voids as in binary or more complex systems (Kim and Yu 2010), the low electromigration effects (Liu et al. 2007), CMOS compatibility and all this at an acceptable material price.

Basically, low temperature bonding processes allow for (i) increased throughput in the wafer bonding system, (ii) improved wafer-to-wafer alignment accuracy after bonding and (iii) optimized device reliability due to thermo–mechanical stress reduction or decreased device degradation. Hence, low temperature Cu–Cu wafer bonding is the process of choice for evaluation.

Within this work preparation techniques and selected analytical techniques for thin metal layer surfaces and interfaces evaluation are presented for the Cu–Cu system. The techniques described here, such as atomic force microscopy (AFM), scanning (SEM) and transmission electron microscopy (TEM), X-ray photoelectron spectroscopy (XPS), Auger electron spectroscopy (AES), secondary ion mass spectrometry (SIMS) and electron backscatter diffraction (EBSD), as well as their corresponding specimen preparation techniques and measurement methodologies, are discussed.

2 Experimental

The 150 mm (otherwise it is mentioned) diameter Si wafers used for experiments were first oxidized using HCl-/O_2-oxidation process (100 nm thick oxide layer, meant to simulate a structure used for real device manufacturing), and then the metal structure was deposited on top of the oxide layer as follows: first 10 nm Ta followed by 20 nm TaN (adhesion/barrier layer) were sputtered, then ~500 nm thick Cu layer was sputtered as bonding layer. For reasons of simplicity these wafers with non-patterned metal layers will be referred further in this work as "Cu wafers". The metal deposition process was performed using an MRC 643 vertical sputtering system.

Especially for low temperature wafer bonding applications a flat wafer surface is very important, too. With reduction of the surface roughness the true contact area, measured on nm-scale, increases, and the remaining interface cavity volume (between the two Cu surfaces after contacting) decreases. With simultaneous chemical and mechanical action, CMP yields surface roughness for Si and also for metals in the nm- and yet sub-nm ranges (Baudin et al. 2011). Directly after CMP treatment the surfaces have to be carefully cleaned to ensure complete removal of particles, slurry residues and organic contaminations (Yeh et al. 2003).

A diluted citric acid ($C_6H_8O_7$—1 wt% in H_2O) treatment was performed ex situ inside the single-wafer cleaning equipment EVG®301 in order to remove the copper native oxide (Pabo et al. 2012). During this reduction process the most stable oxidation state copper(II) oxide, also known as cupric oxide (CuO), was removed by covering the surface 2×2 min while keeping the diluted citric acid at 15 rpm in slight rotational motion (Rebhan et al. 2012). With both, the intermediate and the final de-ionized water rinse and megasonic treatment, effective removal of the solid copper citrate $Cu_3(C_6H_5O_7)_2$ was ensured at 300 rpm and subsequent centrifugation at 2,000 rpm.

After wet chemical treatment the Cu wafers were loaded face-to-face into the EVG®520 semi-automated wafer bonding system to perform in situ forming gas (96 % Ar with 4 % H_2) treatment (after two times evacuation down to 10^{-2} mbar) and the actual Cu–Cu wafer bonding process. During forming gas treatment at the final bonding temperature, the Cu wafers were in 100 μm separation. In order to prevent shifting of the top wafer, the bonding chamber was evacuated to medium vacuum (10^{-2} mbar) prior removing the separation flags and subsequent metal thermo-compression wafer bonding. The bonding was performed 30 min at 175 or 150 °C and typically applying a force of 30 kN, corresponding to a pressure of ~1.7 MPa (otherwise it is mentioned). The subsequent (cheaper) batch annealing process, performed at 200 °C for 1 h, was introduced to establish further grain growth over the interface, while keeping the cycle time in the bonding chamber and hence the cost of ownership at a minimum. It should be added that the heating ramp was 30 °C/min and the time duration of the forming gas treatment was 30 min.

For a successful analysis not only the right technique, but also the specimen preparation is fundamental. The two methods, namely using classical preparation techniques (Gatan method) or focused ion beam (FIB), to successfully prepare a cross-section TEM (X-TEM) image are described below. Proper preparation sequences for other analysis techniques presented in this work can be derived from these approaches. The classical preparation used in this work was facilitated by using a diamond coated saw from Well, a manual grinding machine Varimet from Buehler, the three Gatan systems, Model 601 ultrasonic disc cutter, Model 656 dimple grinder and Model 691 precision ion polishing system (PIPS). For the preparation with FIB, the dual beam system 1,540 XB from ZEISS was used. Additionally it should be mentioned that the preparation of greater regions for cross-section SEM (X-SEM) can be performed with (i) ion x-polishing (Takahashi et al. 2006), (ii) plasma-focused ion beam (plasma-FIB) (Kwakman et al. 1395) and (iii) laser-FIB (Stegmann et al. 2011).

Table 1 Typical specifications of the elemental analysis techniques XPS, AES, EDX, WDX, EELS and SIMS

	XPS	AES	EDX/WDX	EELS (EFTEM)	SIMS
Incident medium	(X-ray) Photon	Electron (SEM)	Electron (SEM)	Electron (TEM)	(Bi) Ion
Incident energy (keV)	~1.4	0.5–30	0.5–30	200	25
What is detected?	(Photo-) Electron	(Auger-) Electron	(Charact.) X-ray	(Primary) Electron	(Secondary) Ion
Detected en./mass	$100 - E_i$[a]	<2.5 keV	$100 - E_i$[a]	E_i[a] "minus" 0–2.5 keV	<1,000 amu
Lat. resolution	15 μm (400) μm	10 nm	100 nm	0.2 nm (10 nm)	250 nm (7 μm)
En./mass resolution	0.05 eV	1–2eV	10–100 eV	0.1–1 eV	10^{-4} at 29 amu
Detection limit	A few %	A few %	A few %	A few %	A few ppm
Depth information	<5 nm	<5 nm	200–2,000 nm	Whole lamella	<5 nm
Quantification[b]	Yes	Yes	Yes	Yes	No
Element range	$Z \geq 3$	$Z \geq 3$	$Z \geq 3$	$Z \geq 3$	$Z \geq 1$

[a] E_i stands for the energy of the incident electron or photon

[b] Standard less

Within this work measurement results gained from SEM and EBSD were obtained by using a dual beam system 1,540 XB from ZEISS, equipped with a GEMINI® field emission electron column and a Nordlys EBSD detector from HKL technology with the "channel 5" software. TEM inspection was performed on a JEM-2010 from JEOL. Further, elemental analysis was operated either on a JAMP-9500F field emission Auger microprobe from JEOL, on an XPS system Theta Probe from ThermoFisher with an Al K$_\alpha$ X-ray source, or on a TOF.SIMS[5] from ION-TOF. Basically, the expression TOF is referred to as time-of-flight and describes the way of how mass spectrometry is performed. For surface roughness determination an atomic force microscopy (AFM) Dimension 3100 from Veeco with a Super Sharp Silicon™ tip called SSS-NCHR-50 was used.

In Table 1 the specifications of all used elemental analysis techniques and additionally of energy (EDX) and wavelength dispersive X-ray spectroscopy (WDX) and electron energy loss spectroscopy (EELS) are listed. The crucial differentiating factors of the individual techniques are the high surface sensitivity of XPS, AES and SIMS, the significantly better detection limit of SIMS, and the high lateral resolution of AES and EELS.

3 Specimen preparation for analysis

In this section the preparation sequences for successful AES, X-SEM, X-TEM and EBSD measurements are described.

Two different types of samples were investigated: blank Cu wafers and bonded Cu–Cu wafers. The use of two fundamentally different types of samples and subsequent analysis require also different specimen preparation methods. The analysis of Cu–Cu bonded specimens first requires that one
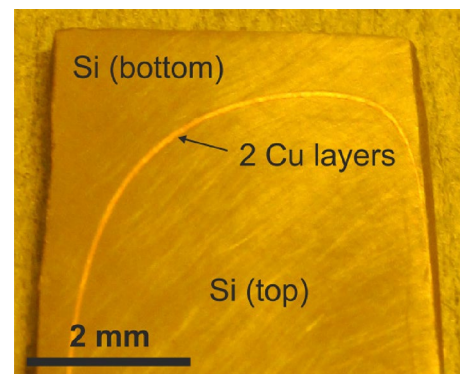

Fig. 1 Cu–Cu bonded specimen after back-grinding and polishing for AES, X-SEM, X-TEM and EBSD measurements

Si side is completely removed or at least thinned back to less than 5 μm to ensure that the subsequent Ar sputtering or FIB milling can reach the actual region of interest: the copper layer(s). This was performed with grinding using grinding pads with SiC particles down to 10 μm, and polishing with diamond particles down to 1 μm until the Cu layers are visible as shown in Fig. 1. Such a back-grinded specimen, with simultaneously accessible thin Si (top) layer, the two intermediate Cu layers and the second Si (bottom) layer, can be prepared with a tiny, finite wedge with relatively small efforts.

This described preparation is used for the further preparation steps of Cu–Cu bonded specimens. For both, the Cu–Cu bonded and the blank Cu specimens, the further preparation and measurement is almost identical.

3.1 AES specimen preparation

Depth profiling in an AES of Cu–Cu bonded layers should start in the thin Si (top) layer and end in the second Si
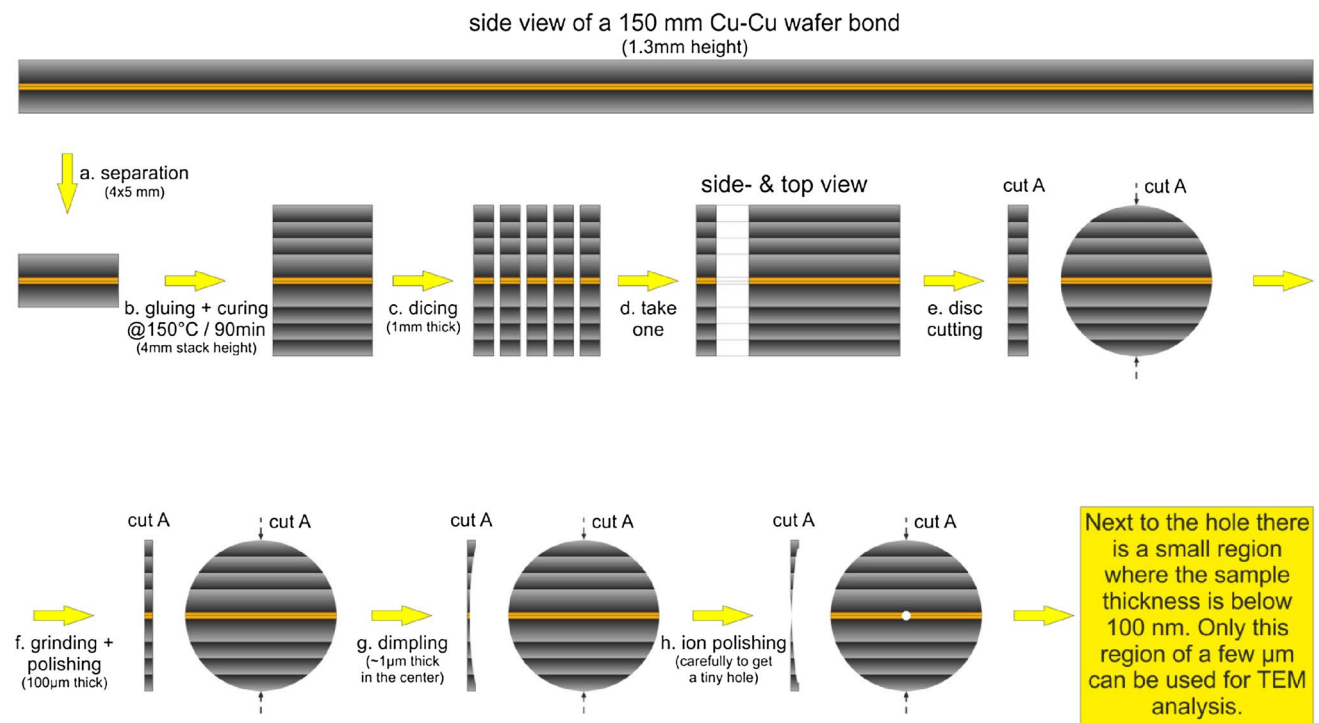
Fig. 2 Schematic view of the Gatan method to prepare the cross-section of a Cu–Cu wafer bonded specimen for TEM. The individual preparation steps are **a** separation, **b** gluing and curing at 150 °C, **c** dicing, **e** disc cutting, **f** grinding and polishing, **g** dimpling and **h** ion polishing

(bottom) layer to gain elemental information of the layer structure Si/SiO₂/Ta/TaN/Cu/interface/Cu/TaN/Ta/SiO₂/Si. Of special interest is the determination of oxygen or e.g. carbon-containing contamination in the bonding interface. This analysis can already be performed using the above described preparation by starting the analysis at a position of the thinned Si (top) layer which is close to the Cu. Here the Si height is typically below 1 μm.

3.2 X-SEM specimen preparation with FIB

X-SEM specimen preparation of Cu–Cu bonded layers is also performed at a position of the thinned Si layer which is close to the Cu region. Before starting to mill a wedge into the bulk material, an overlayer has to be deposited using a gas injection system (GIS) to smoothen the surface in order to eliminate potential scratches caused during grinding and insufficient polishing. Hence, curtaining effects are minimized. After milling a wedge with the FIB, X-SEM is typically performed with in-lens or secondary electron (SE) detector.

For blank Cu wafers the surface can be protected from the ion deposition process by adding either a pen line or an electron-deposited overlayer previously. The later can be deposited using the GIS and simultaneously scanning with the electron beam over the region of interest. Thus, a

moderately deposited overlayer, which does not impact the Cu surface like ions do, can be produced.

Alternatively, an ex situ cross-section polishing system can be used to prepare a polished cross-section suitable for SEM inspection. The cross-section polishing system cannot be used for precisely position-controlled preparations, which in contrast is utilized by the FIB system.

3.3 X-TEM specimen preparation

X-TEM sample preparation is probably the most time-consuming preparation, while having a high risk to irreversibly deteriorate the sample at any preparation step. This applies by either using the Gatan method or by using the FIB. For both methods low-energetic ion treatment (close to the final inspection area) at low incidence angle is crucial. Further, the characterization of wafer pairs bonded at low temperature requires the usage of glues which are cured at low temperature (Gatan method). Besides these two approaches a multitude of other approaches do exist (Avache et al. 2010) and each has a different impact on the measurement result.

3.3.1 Gatan method

With the Gatan method, where the schematic preparation sequence is shown in Fig. 2, TEM samples can be prepared

Fig. 3 Cu–Cu bonded wafer pair prepared with FIB for a X-TEM measurement. First, a 2 × 20 μm² Pt overlayer is deposited (**a**). Then two wedges are milled (**b**), the lamella is almost excluded from the bulk (**c**) before the micro-manipulator is attached (**d**). Then the lamella is completely separated from the bulk and transferred to the TEM Cu-grid (**e**), where it is thinned until it is transparent for electrons with an energy of 3 keV (**f**). The TEM Cu-grid, with its three strips to attach lamellas, is shown in the inset of (**e**)
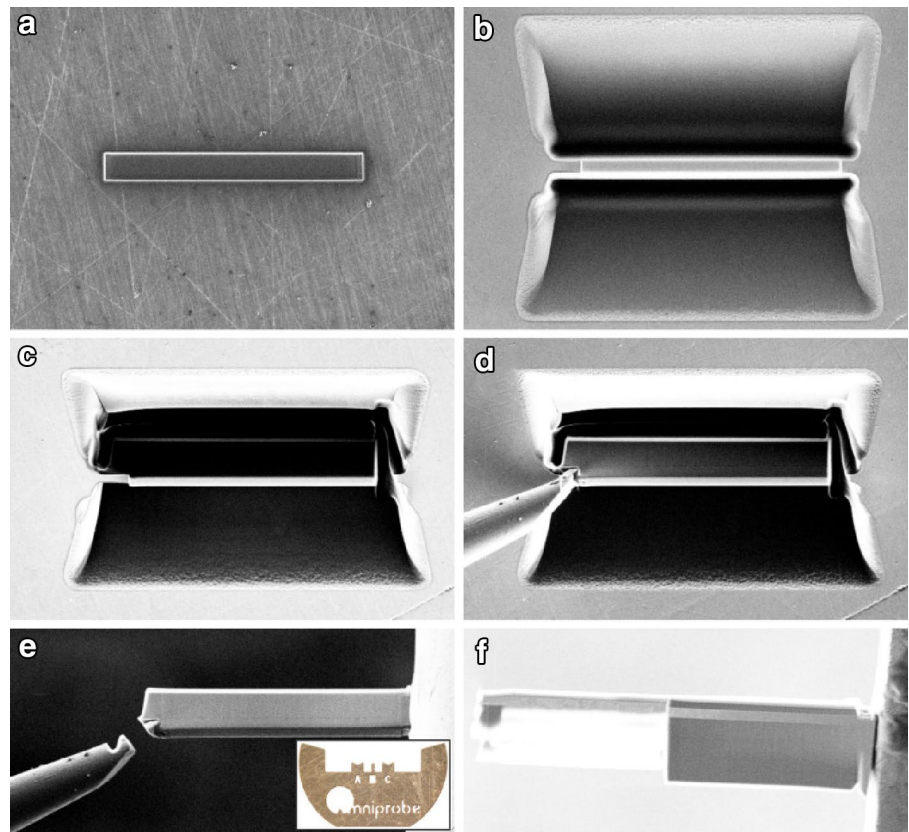
with a geometry which suits for the TEM goniometer (TEM sample holder and manipulator).

The preparation sequence starts with isolation of a 4 × 5 mm² sample by using a diamond-coated saw. Together with other Si wafer pieces it is then stacked using a thermally cured glue, while applying force with a bench vice for 90 min at 150 °C. Afterwards, the diamond-coated saw is used to cut 1 mm thin pieces. At this stage the sample size, with respect to its lateral dimension, is adapted to suit to the TEM goniometer using the ultrasonic disc cutter. Then the disc is carefully thinned down to 100 μm with different grinding pads, and then both sides are polished using 3 and 1 μm diamond particles, subsequently. In the center the thickness is further reduced down to about 10–20 μm using a Cu wheel and a paste with 3 μm polycrystalline diamond particles, followed by dimpling with a polishing fiber wheel and 1 μm polycrystalline diamond particles for polishing until the specimen is transparent for red light. Finally, the dimpled sample is ion polished in a PIPS using an Ar ion beam with 5–20 μA current and 2–3 keV ion energy, while rotating the dimpled sample at a speed of 2–4 rpm to smoothly reduce the thickness in the center region until (almost) a tiny hole is occurring.

It should be mentioned that thermal treatments at 120 °C for a few minutes are frequently applied intermediate steps to fix the sample on the various used sample holders with a so-called specimen mounting wax. These temperature treatments and the thermal treatment for curing (see Fig. 2) represents a drawback of this method as it can change the original low temperature (≤200 °C) Cu–Cu bonded microstructure.

3.3.2 FIB preparation

The FIB method (shown in Fig. 3) can be used for preparation of TEM specimens of almost any material. For Cu–Cu bonded specimens the FIB preparation starts with depositing a 2 × 20 μm² Pt overlayer (see Fig. 3a). At perpendicular incidence (stage is tilted to 54°) two wedges are milled to have access to a strip (lamella) including the Cu layers (see Fig. 3b). Then the stage is rotated back to 10°, where the lamella is almost excluded from the bulk (see Fig. 3c). Then the micro-manipulator is attached to the lamella by using the GIS and the FIB, before the lamella is completely separated from the bulk (see Fig. 3d). With the micro-manipulator the lamella is then transferred to the TEM Cu-grid by gluing the lamella to one of the strips in the center of the Cu-grid (see inset of Fig. 3e) and subsequently separating the micro-manipulator from the lamella by FIB cutting (see Fig. 3e). Out of the lamella the thinning process is performed by forming a sharp wedge which points downwards (see Fig. 3f).
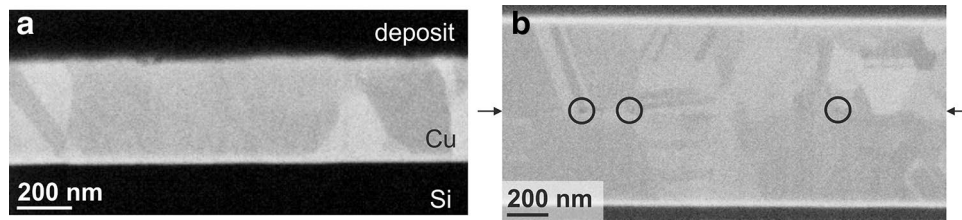
Fig. 4 X-SEM images of **a** a single Cu wafer which was CMP polished and of **b** a bonded Cu–Cu wafer pair. The layer labelled as "deposit" is a pen, used for the protection of the Cu layer during the preparation of the cross-section. In both cases the cross-section was prepared using FIB. In **b** the bonding was performed at 175 °C for 30 min at a bonding force of 27 kN (100 mm wafer size) which corresponds to a bonding pressure of ~3.4 MPa. The arrows indicate the position of the initial bonding interface prior bonding

Therefore the ion beam is adjusted to an incidence angle of 87° and 93° orientated to the side with the Pt overlayer. In the first thinning step the FIB acceleration voltage is 30 kV until the specimen gets electron transparent by using the SE-detector and primary electrons with energy of 5 keV. Afterwards the FIB voltage and the current are reduced to 5 kV and 50 pA, respectively, and the primary electron energy to 3 kV. With this set-up amorphization effects are widely reduced, and the specimen is thinned back until it is electron transparent. The simulation software "the stopping and range of ions in matter" (SRIM) predicts an ion range perpendicular to the polished surface <5 nm. With this last preparation step the Cu-grid with the thinned lamella can be transferred to the TEM goniometer.

Similar as for the X-SEM sample preparation of blank Cu wafers, for X-TEM sample preparation a pen line or an electron-deposited overlayer can be applied.

It has to be accounted for that thinning with high ion energies (30 keV) generates defects (e.g. vacancies) in the first 15 nm (SRIM simulation) and changes the grain structure significantly. If the ion dose is too high, even amorphization of the thin sample may occur and thus the microstructure (grains separated by grain boundaries) is not observable with the TEM anymore.

3.4 EBSD specimen preparation

It is well-known that successful EBSD measurements require specimens with extremely low surface roughness and defect density within the first 30 nm. For blank Cu wafers the surface can be treated with CMP. Single pieces (without CMP treatment) can be manually polished by using "OP-S suspension" from Struers. For thin Cu layers the polishing time should not exceed 5 s, while ensuring low forces (5 N) and adequate rinsing with this suspension, to avoid complete removal of the thin Cu layer. Immediately after polishing the sample surface has to be rinsed with de-ionized water and purged with pressurized air or nitrogen.

4 Results and discussion

4.1 Surface roughness

The surface roughness R_{RMS} was measured during the incoming inspection with AFM on a 2×2 μm^2 area at more than 20 identically processed wafers. The average surface roughness of Cu wafers with and without CMP treatment was measured as 1.84 and 6.18 nm, respectively.

4.2 Morphology

Often the microstructural analysis of deposited films and of bonded layers is performed in an SEM or TEM. TEM offers higher resolution for small feature dimensions, even allowing observation of thin native oxide layers (e.g. 2 nm thick) that can be distinguished from the pure metal layer. Furthermore the grain structure is easier accessible due to (i) the sharp grain boundaries, (ii) the simple identification of the grain orientation in the diffraction mode and (iii) the enhanced grain orientation contrast in dark field mode (see Fig. 6).

As obtaining the X-SEM micrographs is definitely less time-consuming with respect to preparation and measurement procedure and the costs of an SEM equipment are lower compared to a TEM, an SEM is the preferred inspection tool as long as boundaries can be imaged with a high contrast and the structure size can be clearly resolved. In Fig. 4a the X-SEM image of a Cu layer and in Fig. 4b the X-SEM image of a bonded wafers pair are shown. Both samples were prepared with FIB and the images were recorded with (a) an in-lens detector and (b) an SE detector, respectively. Independent on the used detector, from both micrographs only a low contrast between different grain orientations can be observed. Hence the (slight) grain growth over the interface can be obtained only with limitation. The interface cannot be distinguished from the Cu bulk, in case of "zigzag" shaped grain growth over the interface. Hence, the mechanical as well as the electrical contact should be equivalent to that of Cu bulk.

Fig. 5 X-TEM image of **a** a single Cu wafer (with deposited Ta, TaN and Cu layers on Si substrate) which was CMP polished and **b** a highly-resolved TEM image of its native Cu-oxide. The layer labelled as "deposit" is a pen, used for the protection of the Cu layer during the cross-section preparation with FIB
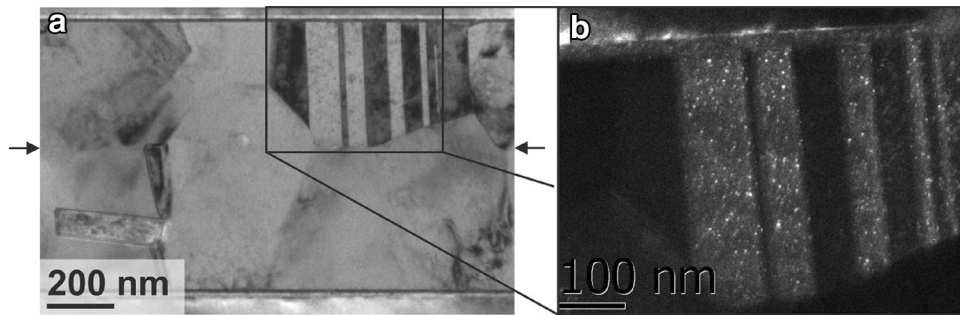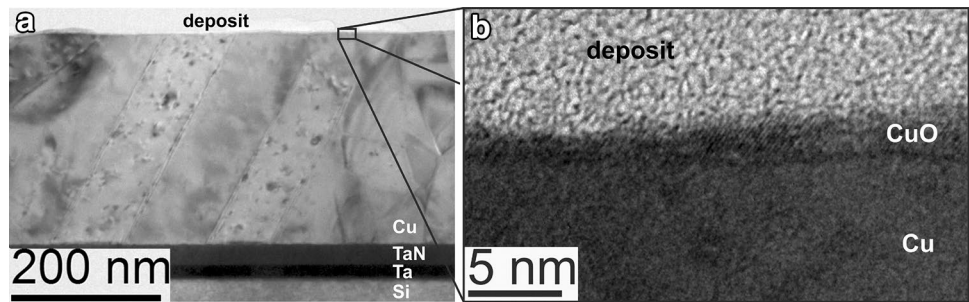

Fig. 6 In **a** the X-TEM image shows a Cu–Cu wafer pair which was bonded at 175 °C for 30 min at a bonding force of 30 kN which corresponds to a bonding pressure of ~1.7 MPa. The arrows indicate the position of the initial bonding interface prior bonding. The preparation was performed with the Gatan method. In **b** a dark field image of the selected region is demonstrated

Nevertheless, some bonding voids located close to the initial bonding interface could be observed. These kinds of bonding voids were also observed when wafers with a finite roughness (such as shown in Fig. 4a) were bonded at room temperature using a direct bonding (contacting at one position, followed by a self-propagating bonding wave) approach (Di Cioccio et al. 2014).

Better suited (but having the drawbacks of time-consuming preparation and inspection as well as increased tooling costs) for high-quality cross-sections is X-TEM imaging. A X-TEM micrograph of a Cu wafer with a highly resolved view of the native copper oxide layer is illustrated in Fig. 5. Here the sample was prepared with the FIB. With the help of selected area diffraction pattern (SADP) (not shown here) the microstructure in Fig. 5a was identified as (Σ3) crystal twinning. From the high-resolution TEM image (HR-TEM) a polycrystalline structure of the native copper oxide, and a thickness of 2.6 ± 0.6 nm were determined. The chemical analysis performed using XPS (see Fig. 9) shows that the copper oxide type of Fig. 5 is CuO.

In Fig. 6 the X-TEM image of a sample prepared with the Gatan method presents a clear grain growth over the initial bonding interface. By selecting a diffraction spot (extracted from the SADP) corresponding to one grain orientation, the intensity for this grain orientation is strongly enhanced compared to all other grain orientations. This dark field microscopy mode supports the identification of different grain orientations, and particularly in the case of Fig. 6b of twin structures, as well as grain growth over the interface.

While the influence of the preparation techniques (either the Gatan or the FIB approach) on the inspected cross-sections is of minor importance for the above Cu–Cu bonded samples, the influence becomes significantly relevant or even dominates for Cu–Cu wafer pairs bonded at temperatures equal or lower than the temperature used for gluing (see Fig. 2b). Hence a micrograph of a Cu–Cu wafer pair which was bonded at 150 °C or less has to be prepared with the FIB and not with the Gatan method. In Fig. 7 the cross-section of a wafer pair bonded at 150 °C for 30 min and
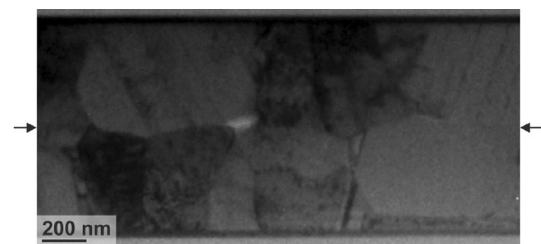

Fig. 7 X-TEM image of a Cu–Cu wafer pair which was bonded at 150 °C for 30 min at a bonding force of 30 kN which corresponds to a bonding pressure of ~1.7 MPa. Post-bond annealing was performed at 200 °C for 1 h. The *arrows* indicate the position of the initial bonding interface prior bonding. The preparation was performed with FIB

subsequently annealed at 200 °C for 1 h shows an interface which has a, compared to the cross-section shown in Fig. 6a, slight "zigzag" shape. Nevertheless, the bonded wafer pair could not be separated using the blade test without breaking the silicon, demonstrating a high Cu–Cu bonding strength. Further, a cavity (or bonding void) can be observed at a position close to the initial bonding interface.

This case is not singular, cavities close to the initial bonding interface were also observed on numerous other TEM as well as SEM cross-sections. It is not completely understood how effectively the ion milling/polishing process influences the size of the void or if some of the observed voids are generated during preparation. The origin of the interfacial voids is currently under discussion. Gondcharton et al. (2014) analyzed three possible reasons for voiding during copper–copper wafer bonding: (i) surface roughness, (ii) oxide presence and (iii) stress-driven vacancy diffusion mechanism. Hence, bonding voids stem from the contacting of two almost planar surfaces. With increasing surface roughness the void size increases. During heat treatment (e.g. in the bonding chamber or oven) the average void size increases while the number of voids decreases; meaning that a number of "small" voids merge into a few "larger" voids in order to minimize the total surface area, and hence the Gibbs free energy of the system. During the preparation of the cross-section these voids probably increase in size and simultaneously e.g. at triple junctions new voids can be generated.

While in the TEM image the barrier layers Ta and TaN as well as the Cu-oxide layer can be investigated, for SEM this is not the case. From the cross-sections it was observed that the contrast of TEM images of adjacent Cu grains is much better compared to the micrographs inspected with SEM. While C-mode scanning acoustic microscopy (C-SAM) can be used to detect voids of 10–50 μm size on the entire wafer, the outcome of X-SEM and X-TEM inspection is a high resolution image but obtain only locally. Usually during failure mode analysis first C-SAM is used for full bonded area inspection and the areas of interest for SEM and TEM investigation are selected based on the acoustic mapping. Typically the cross-sections prepared for SEM and TEM inspection show the bonding interface along a distance of 5 and 20 μm (this is 1/30,000 and 1/7,500 of the 150 mm wafer size), respectively. Hence a cross-section inspection with SEM or TEM reflects the bonding behavior only in the small inspected area, but elsewhere the properties of the bond interface can be different.

In an SEM inspection the grain orientations of the surface can also be measured by using EBSD. It should be mentioned that X-ray diffraction (XRD) is an alternative method to EBSD. While EBSD is a surface sensitive method and provides laterally resolved crystallographic information, XRD provides averaged and more bulk-like data. Typically
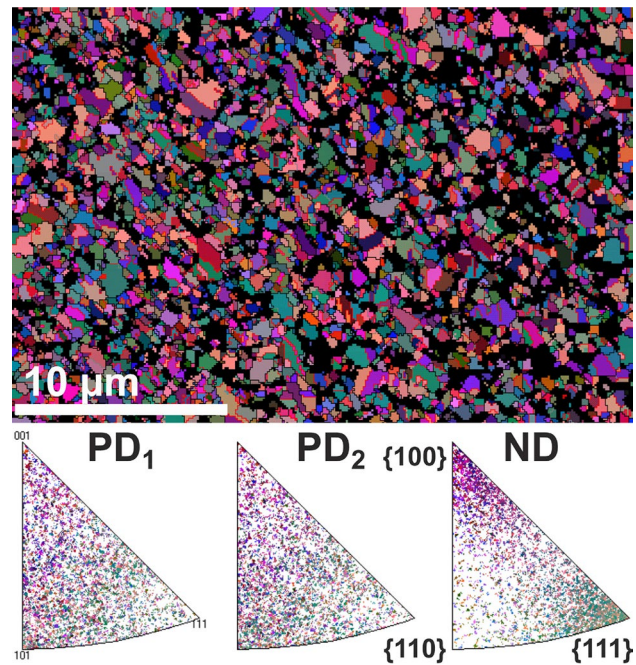

Fig. 8 Orientation mapping (*top*) and IPF (*bottom*) from EBSD measurements of an untreated Cu surface after CMP. From *left* to *right* the IPF are related to the parallel (*lateral*) directions: PD_1 and PD_2, and to the normal direction: ND. Each IPF has the {100}, {110} and {111} orientation in the *top*, in the *bottom left* and in the *bottom right corner*, respectively

with the EBSD evaluation software the distributions of (i) the grain size, (ii) the orientation and (iii) the misorientation angle can be extracted in a simple way. In Fig. 8 the orientation distribution (mapping) with the corresponding inverse pole figures (IPF) of the blank Cu surface is presented. For this sample the preparation was done with CMP (entire wafer). At first, without having a closer look on the two lateral IPF, namely the parallel 1 (PD_1) and parallel 2 direction (PD_2), an almost homogeneous lateral grain orientation distribution can be assumed. Both directions, PD_1 and PD_2, are parallel to the surface, but normal to each other. In the normal (with respect to the surface) direction (ND) the intensity plot (not shown here) shows that the dominating contribution belongs to the {111} orientation, while there are only a few grains with {100} orientation and almost no grains are oriented with the {110} orientation. From the EBSD data the average grain size (diameter of a sphere) was determined as 380 nm. The grain size influences the ratio of volume and grain boundary diffusion, amongst others across the initial bonding interface, and thus has a strong impact on the final microstructure of the bonded wafer pair. Further, the correlated and uncorrelated misorientation angle distributions were determined. The correlated misorientation angle is the misorientation angle of adjacent grains (pixels) and can, for instance, be used in order to quantify the

Fig. 9 XPS spectrum of the Cu 2p peak taken after storage in cleanroom class ISO 5 environment of a Cu layer with its native copper oxide. The curves labelled with "metal" and "CuO" were fitted to the measured "Cu2p" spectrum
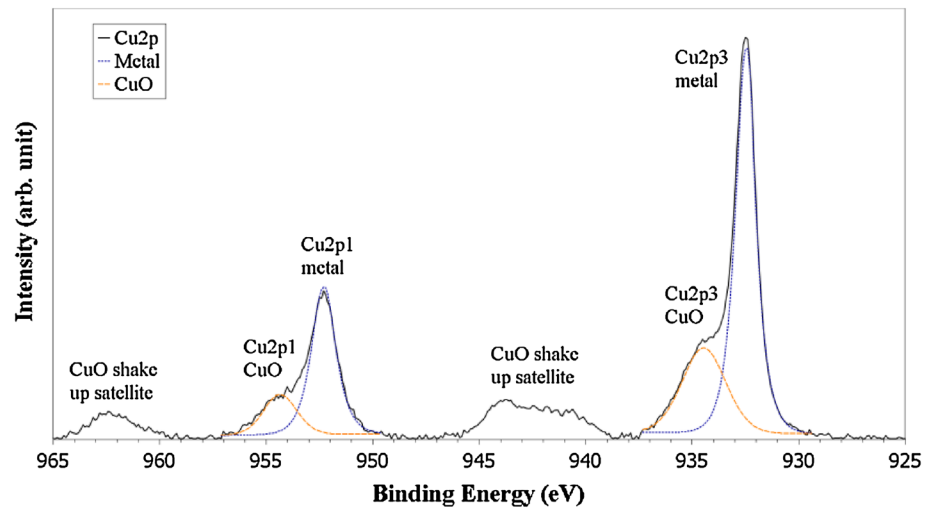
amount of twin boundaries. The result of this measurement was that 30.9 % of the grain boundaries could be identified as $\Sigma 3$ twin boundaries. In comparison to random high-angle grain boundaries, the grain boundary diffusion coefficient of twin boundaries is significantly reduced, and hence the diffusion kinetics during the wafer bonding process is influenced as well.

4.3 Elemental and chemical analysis

Within this section typical measurement applications and the corresponding measurement results of the well-established elemental analysis techniques XPS, SIMS and AES are presented. Compared to the spectra obtained using AES or SIMS, the XPS spectrum is ideally suited for chemical analysis. In Fig. 9 the HR-spectrum of the Cu 2p peak obtained from an XPS measurement of the Cu surface is shown. No explicit preparation (except breaking the wafer into a smaller piece of e.g. 1×1 cm^2) has to be performed to enable this measurement. Besides the sharp lines of the pure metal contribution (Cu 2p1 and Cu 2p3) also peak-broadening in terms of oxide shoulders and shake-up satellites caused by the oxide were recorded. As shake-up satellites can only be obtained for CuO and not for copper(I) oxide, also known as cuprous oxide (Cu$_2$O) the native oxide was identified as CuO. This is in good agreement with the shoulder of the Cu2p3 peak which fits better for the theoretical (Wagner et al. 1979) CuO than for the Cu$_2$O peak. From this it can be concluded that the native copper oxide can be removed with (diluted) citric acid according to the reaction

$$3\,CuO + 2\,C_6H_8O_7 \rightarrow Cu_3(C_6H_5O_7)_2 + 3\,H_2O \qquad (1)$$
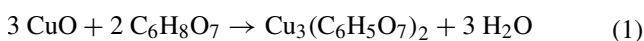
Depth profile spectroscopy is often performed with the combination of a sputtering gun and an AES or XPS, or by using SIMS. Due to the very fast depth profiling mode

and containing information of all isotopes (of one polarity for each measurement), SIMS is a well-suited technique to extract elemental depth-information. As the TOF-analyzer can either only extract positive or negative ions, two measurements, one with the negative and the second with the positive polarity, have to be performed to extract all isotopes, and hence to identify the contribution of all elements. In Fig. 10 the SIMS depth profile of a single Cu wafer after CMP polishing is demonstrated. For this sample the negative polarity already contains the most relevant elemental information. Due to the low ionization probability of nitrogen, the CN$^-$ ion was selected for the determination of nitrogen. A detailed analysis of the Cu bulk purity grade, which corresponds to the isotope measurement in a sputter depth around 80 nm (see Fig. 10), showed that the measured concentrations of impurities (e.g. oxygen, nitrogen, carbon or other metals) were within the noise level of this measurement. SIMS can also be used to measure a survey spectrum, and due to its high mass resolution its sensitivity is in the range of parts per million (ppm) to parts per billion (ppb). Although SIMS has significant benefits compared to alternative elemental analysis techniques, its main drawback is that the quantification procedure is not trivial.
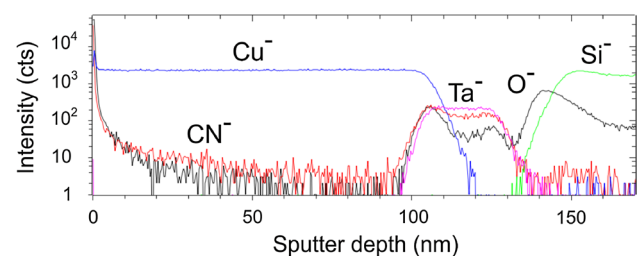

Fig. 10 SIMS depth profile of a Cu wafer after CMP polishing with the measured negative polarity. As nitrogen cannot be detected directly, CN$^-$ is used for its detection
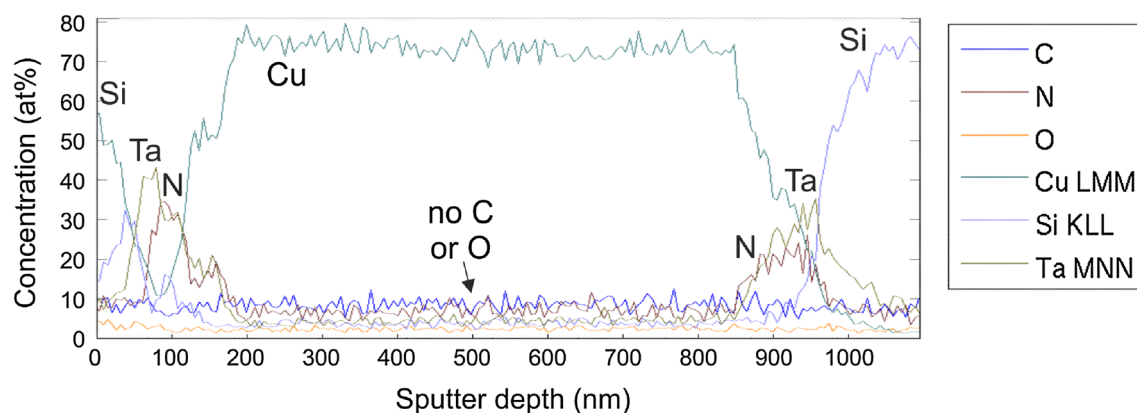
Fig. 11 AES depth profile of a Cu wafer pair bonded at 175 °C for 30 min. The spectrum clearly shows no oxide present in the *initial interface*, indicating a successful oxide reduction. The ending KLL, LMM and MNN are referred to the corresponding electron orbitals prior the Auger process which always consists of three electrons: (i) ejected electron (e.g. K), (ii) electron which moves to the deeper level (e.g. L) and (iii) ejected Auger electron (e.g. L)

For AES (and XPS) measurements the elemental information stems only from the pre-defined elements. In Fig. 11 the AES depth profile of a bonded Cu–Cu wafer pair is presented. The depth profile starts in the Si (top) bulk and ends in the Si (bottom) bulk (see Fig. 1). All in all the elemental contribution of the following layer stack Si/SiO$_2$/Ta/TaN/Cu/interface/Cu/TaN/Ta/SiO$_2$/Si was characterized. The main aim in terms of qualifying the bonding interface is the elemental contribution originating from the bonding interface (corresponding to a sputter depth of ~500 nm). In this case no unwanted "impurities", such as carbon and oxygen, could be detected, hence indicating a successful oxide reduction and no organic contamination prior bonding. In a previous work (Rebhan et al. 2012) a significant concentration of oxygen could be detected by using the same technique. In order to obtain a spatially highly resolved depth profile (i) the surface roughness prior analysis and (ii) the ion acceleration voltage for sputtering has to be kept as low as possible, and (iii) the sample should be continuously rotated during sputtering (Hofmann 2000). Additionally to these three arrangements the depth resolution gets worse with increasing sputter depth. The effect of finite surface roughness and typically used sputter conditions (2 keV Ar ion sputtering for 30 s at 80° sample tilt) can be seen from the peak broadening in the depth profiles shown in Fig. 10 especially for the CN$^-$ and O$^-$ peaks and in Fig. 11 especially for the Ta MNN and N (KLL) peaks.

5 Conclusion

Various analysis techniques, such as AFM, SEM, TEM, EBSD, XPS, AES and SIMS, were applied to characterize the metal layer and bonded metal–metal wafer pair properties, such as surface roughness, morphology and elemental analysis. Within this work Cu was investigated as metal layer for the wafer bonding process, and the experiments were using 150 mm diameter Si wafers sputter-deposited with 500 nm thick Cu layers. The selection of measurements ensured a characterization of the Cu layer as-deposited and of the bonded Cu–Cu wafers feasible to predict or express the quality of the final Cu–Cu wafer bonding interface. With X-TEM it could be shown that bonding of two Cu wafers with a slight "zigzag" shaped grain growth over the interface was feasible even at temperatures down to 150 °C. The surface properties: low surface roughness of and below 6.18 nm and a small average grain size of 380 nm of the deposited Cu-layer were identified. By characterizing the bulk purity grade with SIMS no significant impurities, such as oxygen, nitrogen, carbon and metals, could be found. The elemental composition of the bonding interface demonstrated no evidence of incorporated copper oxide or other impurities. Hence, the surface preparation prior wafer bonding and the selected material setup ensured a high-quality Cu–Cu bonded interface at low bonding temperature. Furthermore, a detailed sample preparation sequence for a subsequent high-quality analysis was described.

References

Avache J, Boumendi J, Beaunier L, Ehret G, Laub D (2010) Sample preparation handbook for transmission electron microscopy: techniques. Springer, Berlin

Baudin F, Di Cioccio L, Moriceau H, Delaye V, Brechet Y (2011) Presented at WaferBond Conf

Chen K, Tan C (2011) IET Comput Digit Tech 5:3

Chen K, Tan C, Fan A, Reif R (2004) Electrochem Solid State Lett 7:1

Di Cioccio L, Baudin F, Gergaud P, Delaye V, Jouneau PJ, Rieutord F, Signamarcheixc T (2014) ECS Trans 64:339

Gondcharton P, Imbert B, Benaissa L, Verdier M (2014) ECS Trans 64:357

Hofmann S (2000) Surf Interface Anal 30:228

Istratova A, Weberb E (2002) J Electrochem Soc 149:1

Kim S, Yu J (2010) J Appl Phy 108:083532

Kwakman L, Franz G, Taklo MMV, Klumpp A, Ramm P (2011) AIP Conf Proc:1395

Liu C, Chen J, Chuang Y, Ke L, Wang S (2007) Appl Phys Lett 90:112114

Moriceau H, Rieutord F, Fournel F, Imbert B, DiCioccio L, Baudin F, Rauer C, Morales C (2012) Presented at LTWB3D Conf

Mounier E, Baron J, Pizzagalli A (2012) Presented at LTWB3D Conf

Pabo E, Rebhan B, Matthias T, Dragoi V (2012) Presented at COMS

Rebhan B, Hesser G, Duchoslav J, Dragoi V, Wimplinger M, Hingerl K (2012) ECS Trans 50:139

Stegmann H, Dömer H, Cai H, Rosenkranz R, Zschech E (2011) Proc. of the 2011 SCD:4

Takahashi H, Sato A, Takakura M, Mori N, Boerder J, Knoll W, Critchell J (2006) Microchim Acta 155:295

Wagner CD, Riggs WM, Davis LE, Moulder JF, Muilenberg GE (1979) Handbook of X-ray photoelectron spectroscopy. Perkin Elmer, Waltham

Yeh C-F, Hsiao C-W, Lee W-S (2003) Appl Surf Sci 216:46